Inorg. Chem. **2008**, *47*, 3841−3850

Relative Axial Ligand Orientation in Bis(imidazole)iron(II) Porphyrinates: Are "Picket Fence" Derivatives Different?

Jianfeng Li,[†] Smitha M. Nair,[†] Bruce C. Noll,[†] Charles E. Schulz,*[,‡] and W. Robert Scheidt*[,†]

Department of Chemistry and Biochemistry, University of Notre Dame, Notre Dame, Indiana 46556, and Department of Physics, Knox College, Galesburg, Illinois 61401

Received December 26, 2007

The synthesis of three new bis(imidazole)-ligated iron(II) picket fence porphyrin derivatives, [Fe(TpivPP)(1-RIm)$_2$] 1-RIm = 1-methyl-, 1-ethyl-, or 1-vinylimidazole) are reported. X-ray structure determinations reveal that the steric requirements of the four α,α,α,α-o-pivalamidophenyl groups lead to very restricted rotation of the imidazole ligand on the picket side of the porphyrin plane; the crowding leads to an imidazole plane orientation eclipsing an iron−porphyrin nitrogen bond. An unusual feature for these diamagnetic iron(II) species is that all three derivatives have the two axial ligands with a relative perpendicular orientation; the dihedral angles between the two imidazole planes are 77.2°, 62.4°, and 78.5°. All three derivatives have nearly planar porphyrin cores. Mössbauer spectroscopic characterization shows that all three derivatives have quadrupole splitting constants around 1.00 mm/s at 100K.

Introduction

Model compound studies of iron(II) and -(III) porphyrinates have been useful for understanding the properties of the hemoproteins.[1] A common goal in many such model compound studies is to develop relationships between structural and spectroscopic features in the expectation that the connections developed can be directly applied to describing and understanding hemoproteins. One area where this strategy has been quite successful has been the examination of the relative and absolute orientation of planar axial ligands. The effect of the axial ligand orientation in iron(III) derivatives is especially clear, whereas the iron(II) porphyrinate systems are less well-understood.

The first example demonstrating the importance of axial ligand orientation was that of [Fe(OEP)(3-ClPy)$_2$]ClO$_4$[2] where two different crystalline polymorphs were isolated.[3−5] In these complexes, the two pyridines maintained a relative parallel orientation, but the absolute orientation of the axial pyridines changes. The differences in the magnetic properties between the two polymorphs can be related to the absolute orientation of the pyridine ligands. In one polymorph, the projection of the axial ligands nearly bisect an N_p-Fe-N_p angle, that is, they are along the iron−meso-carbon directions. A low-spin, high-spin equilibrium ($S = 1/2$, $S = 5/2$) has been found for this polymorph.[4] In the second polymorph, the projection of the two planar axial ligands nearly eclipses an $Fe-N_p$ bond direction, and an intermediate-spin state was found.[5] The differences in physical properties were clearly related to absolute orientation of the axial ligands, and these results led to further study of the effects of axial ligand orientation on the electronic structure of iron porphyrinates.

Subsequent studies on a series of low-spin iron(III) hemes led us to the conclusion that parallel orientations of the two axial ligands, rather than perpendicular orientations, are energetically favored.[6] Low-spin species with axial ligands

* To whom correspondence should be addressed. E-mail: scheidt.1@nd.edu.
[†] University of Notre Dame.
[‡] Knox College.

(1) Walker, F. A. *Chem. Rev.* **2004**, *104*, 589.

(2) The following abbreviations are used in this paper: Porph, a generalized porphyrin dianion; TMP, dianion of meso-tetramesitylporphyrin; TPP, dianion of meso-tetraphenylporphyrin; TTP, dianion of meso-tetratolylporphyrin, TpivPP, dianion of α,α,α,α-tetrakis(o-pivalamidophenyl)porphyrin; TF_5PPBr_8, dianion of 2,3,7,8,12,13,17,18-octabromo-5,10,15,20-tetrakis(pentafluorophenyl)porphyrin; HIm, imidazole; 1-MeIm, 1-methylimidazole; 2-MeHIm, 2-methylimidazole; 4-MeHIm, 4-methylimidazole; 1,2-Me_2Im, 1,2-dimethylimidazole; 1-AcIm, 1-acetylimidazole; 1-$SiMe_3$Im, 1-(trimethylsilyl)imidazole; 1-VinylIm, 1-vinylimidazole; 1-BzylIm, 1-benzylimidazole; RIm, generalized imidazole;Py, pyridine; 3-ClPy, 3-chloropyridine; 4-CNPy, 4-cyanopyridine; 3-CNPy, 3-cyanopyridine; 4-MePy, 4-methylpyridine; 4-NMe_2Py, 4-(dimethylamino)pyridine; Pip, piperidine; Pyz, pyrazine; Im −, imidazolate; 2-MeIm$^-$, 2-methylimidazolate; N_p, porphyrinato nitrogen; N_{ax}, nitrogen of axial ligands; N_{im}, nitrogen of imidazole ligands; EPR, electron paramagnetic resonance.

(3) Scheidt, W. R.; Geiger, D. K. *J. Chem. Soc., Chem. Commun.* **1979**, 1154.

(4) Scheidt, W. R.; Geiger, D. K.; Haller, K. J. *J. Am. Chem. Soc.* **1982**, *104*, 495.

10.1021/ic702498c CCC: $40.75
Published on Web 03/20/2008

having relative parallel orientations display normal rhombic electron paramagnetic resonance (EPR) spectra with three observed g-values consistent with an electronic configuration of $(d_{xy})^2$ $(d_{xz},d_{yz})^3$.[6–10] Bulky axial ligands such as 2-methylimidazole (or, as we later found, the combination of tetrakis-(2,6-disubstituted phenyl)porphyrinates together with pyridines[11,12] or bulky imidazoles[13]), are required to force the relative perpendicular orientation of planar axial ligands in Fe(III) porphyrinates. These iron(III) species display a different EPR spectrum[9,11,13,14] with a single-feature signal at $g \geq 3.2$, that has been called large g_{max}[15] or highly anisotropic low-spin (HALS).[16] For example, for $[Fe(TPP)(2\text{-}MeHIm)_2]^+$,[6,17] the observed spectrum results from mutually perpendicular axial ligands that lead to nearly degenerate iron $d\pi$ (d_{xz},d_{yz}) orbitals.

The application of the principles derived from the combined X-ray and EPR spectroscopic studies of iron porphyrinate derivatives to the hemoproteins with two planar imidazole (histidine) ligands showed that a number of hemoproteins have relative parallel oriented ligands. Systems for which this is shown include cytochromes b_5,[18] three of the heme centers of cytochromes c_3,[19] the b hemes of sulfite oxidase[20] and flavocytochrome b_2,[21] and the heme a of cytochrome oxidase.[22] Other hemoproteins found to have perpendicularly oriented axial ligands based on these developed spectroscopic probes include the b hemes of mitochondrial complex III, also known as cytochrome bc_1,[23] the similar b hemes of cytochrome b_6f of chloroplasts, one of the c-type hemes of cytochrome c_3,[24] and the c-type heme of cytochrome c'' of *Methylophilus methylotrophus*.[25]

Although some effort was required to obtain iron(III) species with perpendicular ligand orientations, we had assumed that for the closed subshell configuration of low-spin d^6 Fe(II) porphyrinates two planar axial ligands would prefer to align themselves in mutually perpendicular planes to maximize the π-bonding interactions between the filled $d\pi$ orbitals of Fe(II) and the π^* orbitals of the ligands. However, subsequent studies[26] showed that obtaining iron(II) derivatives with mutually perpendicular orientations was not as readily achieved as in the iron(III) species. The use of bulky axial ligands and a porphyrin with bulky peripheral groups was required. The structure of $[Fe(TMP)(2\text{-}MeHIm)_2]$ showed that the two axial ligands have a nearly perpendicular ligand orientation and a very ruffled porphyrin core. Mössbauer characterization showed that the complex displayed a large quadrupole splitting of ~1.7 mm/s.[27] These structural and electronic features are markedly different from a series of $[Fe(TPP)(RIm)_2]$ derivatives with parallel orientations and quadrupole splitting of about 1.0 mm/s.[28]

Recently, we synthesized and crystallized the molecule $[Fe(TpivPP)(1\text{-}MeIm)_2]$ as part of a larger study of vibrational dynamics of iron porphyrinates. The X-ray structure of this species revealed that the two imidazole ligands had a relative perpendicular orientation. This unanticipated feature led us to synthesize and characterize two additional picket fence species with different imidazole ligands. These two new species also showed the similar geometric feature of relative perpendicular ligands. All three species were characterized by Mössbauer spectroscopy. These measurements have unequivocally resolved that the effects of porphyrin core conformation rather than axial ligand orientation define the Mössbauer spectra in low-spin iron(II) porphyrinates.

Experimental Section

General Information. All reactions were carried out using standard Schlenk techniques under argon unless otherwise noted. Tetrahydrofuran (THF), benzene, toluene, hexanes, and heptane were distilled over sodium and benzophenone ketyl; all other solvents were used as received (Fisher). $[H_2$ (TpivPP)] and [Fe(TpivPP)Cl] were prepared according to a local modification of the reported synthesis.[29]

Mössbauer measurements were performed on a constant acceleration spectrometer from 4.2 to 298 K with optional small field

(5) Scheidt, W. R.; Geiger, D. K.; Hayes, R. G.; Lang, G. *J. Am. Chem. Soc.* **1983**, *105*, 2625.
(6) Walker, F. A.; Huynh, B. H.; Scheidt, W. R.; Osvath, S. R. *J. Am. Chem. Soc.* **1986**, *108*, 5288.
(7) Blumberg, W. E.; Peisach, J. *Adv. Chem. Ser.* **1971**, *100*, 271.
(8) Scheidt, W. R.; Osvath, S. R.; Lee, Y. J. *J. Am. Chem. Soc.* **1987**, *109*, 1958.
(9) Munro, O. Q.; Serth-Guzzo, J. A.; Turowska-Tyrk, I.; Mohanrao, K.; Shokhireva, T. Kh.; Walker, F. A.; Debrunner, P. G.; Scheidt, W. R. *J. Am. Chem. Soc.* **1999**, *121*, 11144.
(10) Quinn, R.; Valentine, J. S.; Byrn, M. P.; Strouse, C. E. *J. Am. Chem. Soc.* **1987**, *109*, 3301.
(11) Safo, M. K.; Gupta, G. P.; Walker, F. A.; Scheidt, W. R. *J. Am. Chem. Soc.* **1991**, *113*, 5497.
(12) Safo, M. K.; Gupta, G. P.; Watson, C. T.; Simonis, U.; Walker, F. A.; Scheidt, W. R. *J. Am. Chem. Soc.* **1992**, *114*, 7066.
(13) Munro, O. Q.; Marques, H. M.; Debrunner, P. G.; Mohanrao, K.; Scheidt, W. R. *J. Am. Chem. Soc.* **1995**, *117*, 935.
(14) Inniss, D.; Soltis, S. M.; Strouse, C. E. *J. Am. Chem. Soc.* **1988**, *110*, 5644.
(15) Walker, F. A.; Reis, D.; Balke, V. L. *J. Am. Chem. Soc.* **1984**, *106*, 6888.
(16) Magita, C. T.; Iwaizumi, M. *J. Am. Chem. Soc.* **1981**, *103*, 4378.
(17) Scheidt, W. R.; Kirner, J. L.; Hoard, J. L.; Reed, C. A. *J. Am. Chem. Soc.* **1987**, *109*, 1963.
(18) Mathews, F. S.; Czerwinski, E. W.; Argos, P. In *The Porphyrins*; Dolphin, D., Ed.; Academic Press: New York, 1979; Vol. *VII*, pp 107–147.
(19) Czjzek, M.; Payan, F.; Haser, R. *Biochimie* **1994**, *76*, 546.
(20) Kipke, C. A.; Cusanovich, M. A.; Tollin, G.; Sunde, R. A.; Enemark, J. H. *Biochemistry* **1988**, *27*, 2918.
(21) (a) Xia, Z.-X.; Shamala, N.; Bethge, P. H.; Lim, L. W.; Bellamy, H. D.; Xuong, N. H.; Lederer, F.; Mathews, F. S. *Proc. Natl. Acad. Sci. U.S.A.* **1987**, *84*, 2629. (b) Dubois, J.; Chapman, S. K.; Mathews, F. S.; Reid, G. A.; Lederer, F. *Biochemistry* **1990**, *29*, 6393.
(22) Iwata, S.; Ostermeier, C.; Ludwig, B.; Michel, H. *Nature* **1995**, *376*, 660.
(23) (a) Salerno, J. C. *J. Biol. Chem.* **1984**, *259*, 2331. (b) Tsai, A.; Palmer, G. *Biochim. Biophys. Acta* **1982**, *681*, 484. (c) Tsai, A.-H.; Palmer, G. *Biochim. Biophys. Acta* **1983**, *722*, 349.
(24) (a) Pierrot, M.; Haser, R.; Frey, M.; Payan, F.; Astier, J.-P. *J. Biol. Chem.* **1982**, *257*, 14341. (b) Higuchi, Y.; Kusunoki, M.; Matsuura, Y.; Yasuoka, N.; Kakudo, M. *J. Mol. Biol.* **1984**, *172*, 109.
(25) (a) Berry, M. J.; George, S. J.; Thomson, A. J.; Santos, H.; Turner, D. L. *Biochem. J.* **1990**, *270*, 413. (b) Costa, H. S.; Santos, H.; Turner, D. L.; Xavier, A. V. *Eur. J. Biochem.* **1992**, *208*, 427. (c) Costa, H. S.; Santos, H.; Turner, D. L. E. *J. Biochem.* **1993**, *215*, 817.
(26) Safo, M. K.; Nesset, M. J. M.; Walker, F. A.; Debrunner, P. G.; Scheidt, W. R. *J. Am. Chem. Soc.* **1997**, *119*, 9438.
(27) Hu, C.; Noll, B. C.; Schulz, C. E.; Scheidt, W. R. *Inorg. Chem.* **2005**, *44*, 4346.
(28) Safo, M. K.; Scheidt, W. R.; Gupta, G. P. *Inorg. Chem.* **1990**, *29*, 626.
(29) Collman, J. P.; Gagne, R. R.; Halbert, T. R.; Lang, G.; Robinson, W. T. *J. Am. Chem. Soc.* **1975**, *97*, 1427.

Table 1. Complete Crystallographic Details for [Fe(TpivPP)(1-MeIm)$_2$]·1-MeIm, [Fe(TpivPP)(1-EtIm)$_2$]·0.5C$_7$H$_8$, and [Fe(TpivPP)(1-VinylIm)$_2$]·2C$_7$H$_8$

	[Fe(TpivPP)(1-MeIm)$_2$]·1-MeIm	[Fe(TpivPP)(1-EtIm)$_2$]·0.5C$_7$H$_8$	[Fe(TpivPP)(1-VinylIm)$_2$]·2C$_7$H$_8$
chemical formula	$C_{76}H_{82}FeN_{14}O_4$	$C_{77.5}H_{84}FeN_{12}O_4$	$C_{88}H_{92}FeN_{12}O_4$
fw	1311.41	1303.44	1437.59
a, Å	13.2358(3)	13.1799(3)	13.4924(4)
b, Å	19.2487(5)	13.3672(3)	28.2916(9)
c, Å	27.4149(6)	22.2734(5)	20.2542(6)
α, deg	90	75.524(1)	90
β, deg	103.782(1)	88.168(1)	106.108(2)
γ, deg	90	65.322(1)	90
V, Å^3	6783.5(3)	3440.79(13)	7427.9(4)
space group	$P2_1/c$	$P\bar{1}$	$P2_1/c$
Z	4	2	4
temp, K	100	100	100
D_{calcd}, g cm^{-3}	1.284	1.258	1.286
μ, mm^{-1}	0.284	0.279	0.265
final *R* indices	$R_1 = 0.0585$	$R_1 = 0.0444$	$R_1 = 0.0555$
[$I > 2\sigma(I)$]	$wR_2 = 0.1513$	$wR_2 = 0.1114$	$wR_2 = 0.1372$
final *R* indices	$R_1 = 0.0787$	$R_1 = 0.0662$	$R_1 = 0.0796$
(all data)	$wR_2 = 0.1673$	$wR_2 = 0.1297$	$wR_2 = 0.1476$

(Knox College). Samples for Mössbauer spectroscopy were prepared by immobilization of the crystalline material in Apiezon M grease.

Synthesis of [Fe(TpivPP)(1-MeIm)$_2$]·1-MeIm. [Fe(TpivPP)Cl] (55 mg, 0.05 mmol) and fresh zinc amalgam (10% zinc, 1 mL) were dried in vacuum for 30 min. 1-Methylimidazole (0.04 mL) and toluene (∼15 mL) were then transferred into the Schlenk by cannula. This mixture was stirred under an argon atmosphere at 30–40 °C for 2 h. After standing overnight, this red solution was filtered. Hexanes were then allowed to diffuse slowly into the filtrate. One week later, a needle crystalline product was collected.

Synthesis of [Fe(TpivPP)(1-EtIm)$_2$]·0.5C$_7$H$_8$. Similar reaction procedures as above were performed, heptane was used as the nonsolvent to diffuse into the reaction solution. Several days later, a block crystalline product was collected.

Synthesis of [Fe(TpivPP)(1-VinylIm)$_2$]·2C$_7$H$_8$. Similar reaction procedures as above were performed; hexanes were used as the nonsolvent to diffuse into the reaction solution. Several days later, a block crystalline product was collected.

X-ray Structure Determinations. Single crystal experiments were carried out on Bruker Apex II systems with graphite-monochromated Mo Kα radiation ($\lambda = 0.71073$ Å). The crystalline samples were placed in inert oil, mounted on a glass pin, transferred to the cold gas stream of the diffractometer, and crystal data collected at 100 K. The structures were solved by direct methods (SHELXS-97)[30] and refined against F^2 using SHELXL-97.[31,32] Subsequent difference Fourier syntheses led to the location of all remaining nonhydrogen atoms. For the structure refinement, all data were used including negative intensities. All nonhydrogen atoms were refined anisotropically if not remarked upon otherwise below. Hydrogen atoms were idealized with the standard SHELX idealization methods. The program SADABS[33] was applied for the absorption correction. Complete crystallographic details, atomic coordinates, anisotropic thermal parameters, and fixed hydrogen atom coordinates are given in the Supporting Information Tables for all three structures; a brief sumary of crystallographic details is given in Table 1.

(30) Sheldrick, G. M. *Acta Crystallogr.* **1990**, *A46*, 467.
(31) Sheldrick, G. M. *Program for the Refinement of Crystal Structures*; Universität Göttingen: Germany, 1997.
(32) The conventional *R*-factors R_1 are based on *F*, with *F* set to zero for negative F^2. The criterion of $F^2 > 2\sigma(F^2)$ was used only for calculating R_1. *R*-factors based on F^2 (wR_2) are statistically about twice as large as those based on *F*, and *R*-factors based on ALL data will be even larger.
(33) Sheldrick, G. M. *Program for Empirical Absorption Correction of Area Detector Data*; Universität Göttingen: Germany, 1996.

[Fe(TpivPP)(1-MeIm)$_2$]·1-MeIm. A translucent red needle crystal with the dimensions of 0.32 × 0.21 × 0.18 mm^3 was used for the structure determination. The asymmetric unit contains one bis-ligated "picket fence" porphyrin complex and one 1-methylimidazole molecule. One of the tert-butyl groups on the four pivalamide "pickets" was disordered. Thus, the four butyl tert-carbon atoms are restrained by "similar U_{ij}" (SIMU) to constrain the anisotropic displacement parameters.

[Fe(TpivPP)(1-EtIm)$_2$]·0.5C$_7$H$_8$. A dark purple block crystal with the dimensions of 0.32 × 0.19 × 0.10 mm^3 was used for the structure determination. The asymmetric unit contains one bis-ligated "picket fence" porphyrin complex and half of a toluene solvent molecule. The toluene molecule was disordered around an inversion center; thus, the occupancy of the methyl group is refined as 0.5, and the three ring carbons were refined as 1.0.

[Fe(TpivPP)(1-VinylIm)$_2$]·2C$_7$H$_8$. A translucent red plate crystal with the dimensions of 0.28 × 0.16 × 0.12 mm^3 was used for the structure determination. The asymmetric unit contains one bis-ligated "picket fence" porphyrin complex and two toluene solvent molecules. Two of the carbon atoms (C6 and C7) on one of the imidazole rings (C6−C7−N8−C8−N7) exhibited unusual thermal motions suggesting some small disorder that could not be successfully modeled further.

Results

The synthesis, molecular structures, and Mössbauer spectra of three new six-coordinate bis-imidazole "picket fence" porphyrinates, [Fe(TpivPP)(1-MeIm)$_2$]·1-MeIm, [Fe(TpivPP)(1-EtIm)$_2$]·0.5C$_7$H$_8$, and [Fe(TpivPP)(1-VinylIm)$_2$]·2C$_7$H$_8$ are reported. Crystalline [Fe(TpivPP)(1-MeIm)$_2$]·1-MeIm contains one bis-ligated iron porphyrinate and one 1-methylimidazole molecule. Two labeled Oak Ridge thermal ellipsoid plot (ORTEP) diagrams of [Fe(TpivPP)(1-MeIm)$_2$] are given in Figures 1 and 2.

ORTEP diagrams of the molecular structures of the other two bis-ligated "picket fence" iron porphyrinates, [Fe(TpivPP)(1-EtIm)$_2$] and [Fe(TpivPP)(1-VinylIm)$_2$], are shown in the Supporting Information Figures S1−S4. A brief summary of the crystallographic data is given in Table 1, and the complete crystallographic details, atomic coordinates, bond distances, bond angles of these three structure are given in the Supporting Information Tables S1−S18.

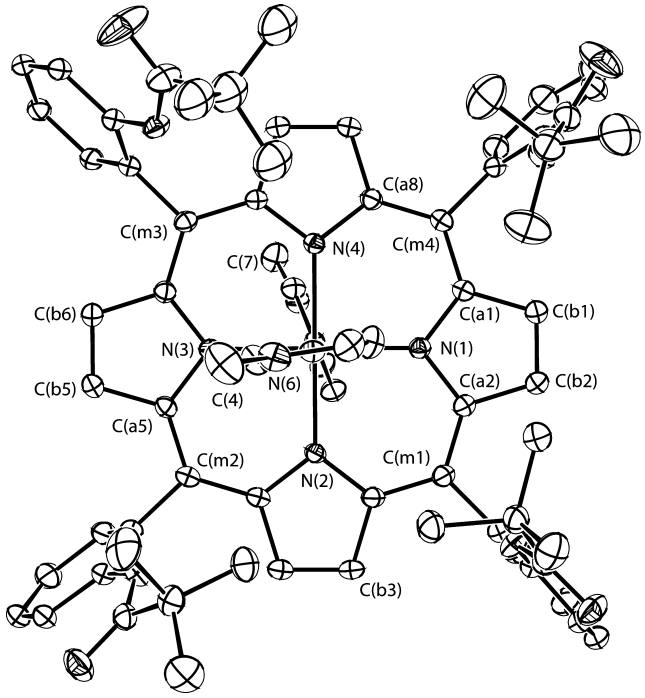

Figure 1. ORTEP diagram of [Fe(TpivPP)(1-MeIm)$_2$] displaying the atom labeling scheme. Thermal ellipsoids of all atoms are contoured at the 50% probability level. Hydrogen atoms have been omitted for clarity. The porphyrin plane is in the plane of the paper.

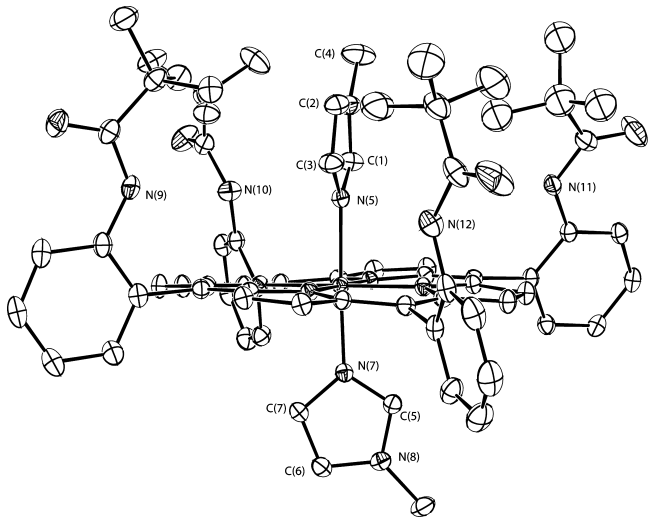

Figure 2. A edge-on ORTEP diagram of [Fe(TpivPP)(1-MeIm)$_2$] displaying the atom labeling scheme. Thermal ellipsoids of all atoms are contoured at the 50% probability level. Hydrogen atoms have been omitted for clarity. The porphyrin plane is perpendicular to the plane of the paper.

Solid-state Mössbauer spectra were measured for all three complexes and taken at several different temperatures from 20 to 298 K; they will be discussed subsequently.

Discussion

Structures. The bis(imidazole)-ligated iron(II) "picket fence" porphyrinates were first presented by Collman and co-workers[29] in 1975 as part of their well-known work on "synthetic models of oxygen-binding hemoproteins." However, no member of the bis(imidazole)-ligated set of species has ever been structurally studied. Recently, we synthesized and crystallized [Fe(TpivPP)(1-MeIm)$_2$] as part of a larger study of vibrational dynamics of iron porphyrinates. The structure determination of this complex showed unexpected and noteworthy features.

Two ORTEP diagrams of [Fe(TpivPP)(1-MeIm)$_2$] have been presented—Figure 1 gives the view normal to the porphyrin plane, whereas Figure 2 is the edge-on view. It can be readily noted that the two imidazole ligands are both perpendicular to the porphyrin plane, and surprisingly, the two imidazole planes have a relative perpendicular orientation. The actual dihedral angle between the two imidazole planes is 77.2°. The two axial imidazole ligand planes almost align with the Fe−N_p axes, with the 1-MeIm ligand planes on the "picket fence" side making a dihedral angle of 8.5°; and the imidazole on the other side making a 21.1° angle to the closest Fe−N_p vector. Additional quantitative information is given in the top panel of Figure 3, which displays the detailed displacements of each porphyrin core atom (in units of 0.01 Å) from the 24-atom mean plane. The orientation of the two 1-MeIm ligands including the values of the dihedral angles are also shown; the circle represents the position of the methyl group on each ligand.

Figure 3 also shows that the core conformation of [Fe(TpivPP)(1-MeIm)$_2$] has a modestly ruffled deformation, with two of the meso-carbon atoms having displacements of 0.14 and 0.15 Å from the mean plane. The iron center is slightly out of the mean plane (0.04 Å) toward the picket side of the porphyrin plane; the average N_p−Fe−N_p angle is ideal at 90.00(18)°. The average Fe−N_p distance of 1.9924(28) Å is a typical value for low-spin (porphinato)iron(II) derivatives.[34]

Although most of these structural features are expected for low-spin bis(imidazole) derivatives, one feature was quite unexpected: the relative perpendicular orientation of the two imidazole rings. To ascertain if this is a general feature of picket fence porphyrin derivatives, we characterized two additional examples with 1-ethyl- or 1-vinylimidazole as the axial ligands. [Fe(TpivPP)(1-EtIm)$_2$]·0.5C_7H_8 and [Fe(TpivPP)(1-VinylIm)$_2$]·2C_7H_8 were thus synthesized and structurally characterized. ORTEP diagrams for both are available in the Supporting Information.

As can be seen from both the ORTEP drawings and the formal diagrams given in Figure 3, the pattern of the orientation of the two imidazoles in these new species is very similar to that seen in [Fe(TpivPP)(1-MeIm)$_2$]. Both ligand planes have a roughly eclipsed orientation with a closest Fe−N_p axis in all derivatives. Moreover, all derivatives have the two axial imidazoles with relative perpendicular orientations. Both derivatives also have modestly saddled core conformations but with a different orientation with respect to the axial ligands. We can conclude from this that the axial ligand must have very little effect on the overall core conformation, but the porphyrin substituents must have significant effects on the axial ligand orientations.

There are several common structural features observed for the three new structures. First, as already noted, the two axial ligands are close to eclipsing the closest Fe−N_p vector, and

(34) Scheidt, W. R.; Reed, C. A. *Chem. Rev.* **1981**, *81*, 543.

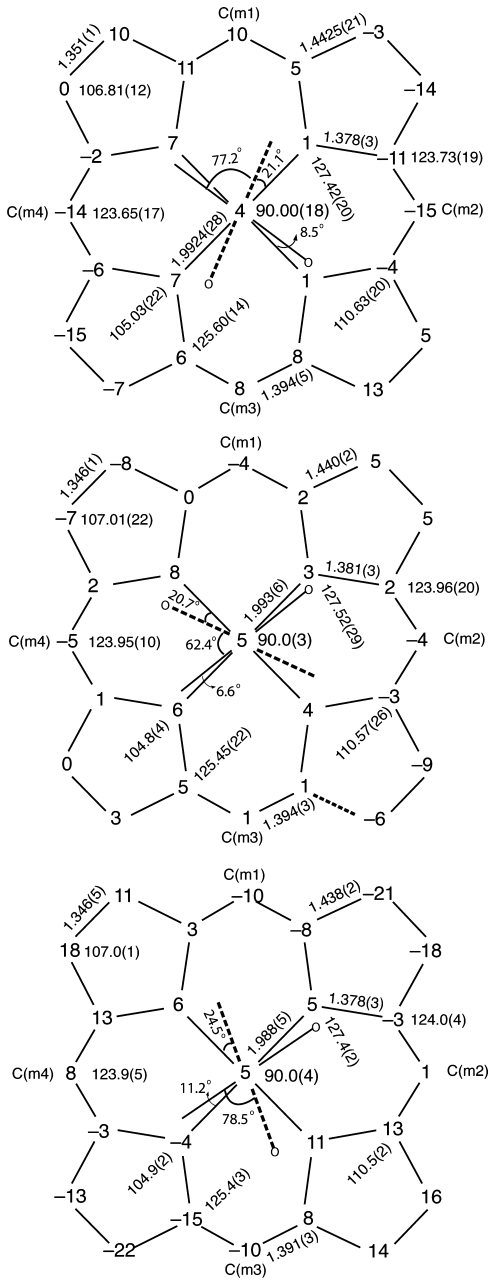

Figure 3. Formal diagrams of the porphinato cores of [Fe(TpivPP)(1-MeIm)$_2$] (top), [Fe(TpivPP)(1-EtIm)$_2$] (middle), and [Fe(TpivPP)(1-VinylIm)$_2$] (bottom). Averaged values of the chemically unique bond distances (in Å) and angles (in degrees) are shown. The numbers in parentheses are the esd's calculated on the assumption that the averaged values were all drawn from the same population. The perpendicular displacements (in units of 0.01 Å) of the porphyrin core atoms from the 24-atom mean plane are also displayed. In all diagrams, positive values of the displacement are towards the hindered porphyrin side while the dashed line indicates the imidazole on the unhindered porphyrin side.

second, the two axial ligands have relative perpendicular orientations. Third, the central iron atom has a small out-of-plane displacement of 0.04 to 0.05 Å with all displacements toward the hindered (picket) porphyrin side. Fourth, the imidazole plane on the hindered side always has a smaller dihedral angle with the closest Fe−N_p axis. Thus, the three structures have dihedral angles in the range of 6.6−11.2° on the picket side, and 20.7–24.5° on the other side. The Fe−N_{ax} distances on the picket side are slightly elongated compared to those of the unhindered side. The differences are 0.004 Å in ([Fe(TpivPP)(1-MeIm)$_2$]), 0.030 Å in ([Fe(TpivPP)(1-EtIm)$_2$]), and 0.011 Å in ([Fe(TpivPP)(1-VinylIm)$_2$]). This bond length asymmetry, especially prominent in iron(III) species, had been explained by the nonbonded interactions between coordinated imidazole and porphinato atoms.[35,36]

The key structural parameters of all structurally characterized [Fe(II)(Porph)(L)$_2$] structures with "L" being a nitrogen donor axial ligand are shown in Table 2. All but one of these derivatives have planar axial ligands. Listed in the table is the crystallographically required symmetry at the iron center, the absolute ligand orientation given by the dihedral angle between the axial ligand plane and the closest N_{ax}−Fe−N_p plane, conventionally denoted by φ. Also given is the relative ligand orientation, the dihedral angle between the two axial ligand planes and denoted by θ.

Excluding the current derivatives, there are a total of 16 reported iron(II) structures in Table 2. Ten of these have crystallographically required inversion symmetry at iron and necessarily have relative parallel axial ligand pairs. The last six species of Table 2 have no symmetry at iron (five) or C_2 symmetry (one). Most have relatively large values of the dihedral angle between the two axial ligands. Are there explanations for the six derivatives that are different from those for the ten derivatives? We believe that the differences appear to reflect the contrast in core conformation. The ten derivatives with relative parallel axial ligand orientations also have near planar porphyrin cores consonant with the observed inversion symmetry, whereas the six derivatives with nonzero dihedral angles between the two axial ligands have strongly ruffled or saddled porphyrin core conformations that do not allow the possibility of an inversion center. A combination of porphyrin peripheral groups, porphyrin core conformation, and/or axial ligand substitution in these six derivatives are the reason for the absence of the inversion center. We consider the stereochemical features of these derivatives in turn.

In six-coordinate [Fe(TMP)(2-MeHIm)$_2$], a near-perpendicular relative ligand orientation results from coordination of two bulky 2-methylimidazole axial ligands.[27] The 2-methyl groups of the axial ligands induce a strongly ruffled porphyrin core in which the ligands must bind in mutually perpendicular ligand binding pockets if the species is to become low spin. The sterically crowded system leads to slight increases in the axial Fe−N_{Im} bond distances relative to the other imidazole derivatives in Table 2. An electronic reason for ruffling is precluded in these structures as the low-spin d^6 electron configuration minimizes possible porphyrin → Fe π donation. This is in contrast to the Fe(III) case where Por→Fe(III) π donation from the porphyrin a_{2u} (π) orbital requires ruffling[26,37,38] when the ground-state is $(d_{xz},d_{yz})^4(d_{xy})^1$.

Two additional examples have near-perpendicular ligand orientation: [Fe((C$_3$F$_7$)$_4$)P)(Py)$_2$][39] and [Fe(TF$_5$PPBr$_8$)(Py)$_2$].[40] These two complexes have extremely ruffled ([Fe((C$_3$F$_7$)$_4$)P)(Py)$_2$]) or saddled ([Fe(TF$_5$PPBr$_8$)(Py)$_2$]) core

(35) Scheidt, W. R.; Chipman, D. M. *J. Am. Chem. Soc.* **1986**, *108*, 1163.

Table 2. Selected Structural Parameters for [Fe(II)(Porph)$(L)_2$][a]

complex	Fe S. S.[b]	$(Fe-N_p)_{av}$[c,d]	$Fe-N_{ax}$[d]	core conf.[d,e]	$\varphi_{1,2}$[f,g]	θ[f,h]	ref.
[Fe(TpivPP)(1-MeIm)$_2$]	C_1	1.992(3)	1.9958(19)	near-Pla	8.5	77.2	tw
			1.9921(18)	(C_m,0.12)	21.1		
[Fe(TpivPP)(1-EtIm)$_2$]	C_1	1.993(6)	2.0244(18)	near-Pla	6.6	62.4	tw
			1.9940(19)	(C_β,0.05)	20.7		
[Fe(TpivPP)(1-VinylIm)$_2$]	C_1	1.988(5)	1.9979(19)	Near-Pla	11.2	78.5	tw
			1.9866(18)	(C_β,0.17)	24.5		
[Fe(TPP)(1-VinylIm)$_2$]	C_i	2.001(2)	2.004(2)	near-Pla	14	0[i]	28
[Fe(TPP)(1-BzylIm)$_2$]	C_i	1.993(9)	2.017(4)	near-Pla	26	0[i]	28
[Fe(TPP)(1-MeIm)$_2$]	C_i	1.997(6)	2.014(5)	near-Pla	15	0[i]	42
[Fe(TPP)(4-MeHIm)$_2$]	C_i	1.9952(8)	2.0154(8)	near-Pla	0.7	0[i]	43
[Fe(TMP)(4-CNPy)$_2$]	C_i	1.993(2)	1.996(2)	near-Pla	40	0[i]	26
[Fe(TMP)(3-CNPy)$_2$]	C_i	1.996(2)	2.026(2)	near-Pla	42	0[i]	26
[Fe(TMP)(4-MePy)$_2$]	C_i	1.988(2)	2.010(2)	near-Pla	41	0[i]	26
[Fe(TPP)(Py)$_2$] Py	C_I	1.993(6)	2.039(1)	near-Pla	34.4	0[i]	44
[Fe(TPP)(Py)$_2$]	C_i	2.001(2)	2.037(1)	near-Pla	45	0[i]	45
[Fe(TPP)(Pip)$_2$]	C_i	2.004(6)	2.127(3)	near-Pla		0[i]	46
[Fe(TMP)(2-MeHIm)$_2$]	C_i	1.964(5)	2.030(3)	Ruf(0.51)	41.1	82.4	27
(mol 1)			2.047(3)		41.4		
[Fe(TMP)(2-MeHIm)$_2$]	C_1	1.961(7)	2.032(3)	Ruf(0.50)	44.8	84.4	27
(mol 2)			2.028(3)		37.9		
[Fe($(C_3F_7)_4$)P)(Py)$_2$]	C_1	1.958(4)	2.007(6)	Ruf(0.62)	41.3	87.5	39
			1.996(6)		46.0		
[Fe(TF_5PPBr_8)(Py)$_2$]	C_1	1.963(4)	2.007(7)	Sad(0.97)	1.5	68.3	40
			2.016(7)		22.2		
[Fe($TPPBr_4$)(Py)$_2$]	C_2	1.976(2)	2.000(3)	Sad(0.67)	36.8	19.2	47
			2.040(3)		33.7		
[Fe(TPP)(Pyz)$_2$]	C_1	1.987(8)	2.010(3)	Sad(0.14)	3.9	40.9	48
			1.970(3)		37.0		

[a] Estimated standard deviations are given in parentheses. [b] Site symmetry of Fe. [c] Averaged value. [d] Value in Å. [e] Number in parenthesis is the average displacement of the methine carbons (C_m) or pyrrole β carbons (C_β) from the 24-atom mean plane for ruffling (Ruf) or saddling (Sad) deformation, respectively; near-Pla indicates an almost planar porphyrin plane in a centrosymmetric or picket fence structure. [f] Value in degrees. [g] Dihedral angle between the plane of the closest N_p-Fe-N_{ax} and the ligand plane. [h] Dihedral angle between two axial ligands. [i] Exact value required by symmetry.

conformations. These core conformations are the result of the peripheral substituents. The final two examples have smaller dihedral angles between the two axial ligands; however, only the last example could actually have inversion symmetry for the molecule as a whole.

The picket fence derivatives are another set of porphyrin systems that lead to relative perpendicular orientations of the two axial ligands in iron(II) species; however, the basis for this effect appears to be distinct from any of the systems given above.

We start with an examination from the hindered porphyrin side of the molecules. The "picket fence" environment has strong steric effects on the axial ligand orientation. The crowding between the four bulky t-butyl groups of the pickets and the axial imidazole will allow only a limited rotational motion of the axial ligand around the $Fe-N_{Im}$ bond. This crowding forces the axial ligands to align in specific orientations, always near the axes defined by the porphyrin nitrogen atoms, and prevents the imidazoles from freely rotating. The three different imidazoles on the picket side all show very small dihedral angles with the closest $Fe-N_p$ axis (φ): 8.5° (1-MeIm), 6.6° (1-EtIm), and 11.2° (1-VinylIm). This effect is clearly illustrated by the space-filling models shown in Figure 4 for the three species. A close examination of the t-butyl group orientations in the three species shows that there are small differences that reflect the differing sizes of the axial imidazoles. This is most clearly seen in the differences between the 1-vinylimidazole species and the other two; in the vinylimidazole system, the pickets form two "walls" rather than the "V-shaped" cavity of the other two derivatives.

We then need to consider the orientation of the second imidazole on the opposite, unhindered porphyrin side. As shown in the three 24-atom mean plane diagrams (Figure 3), the second imidazoles all have small φ angles ranging from 20.7 to 24.5° with the closest $Fe-N_p$ axis. Space-filling models showing the opposite side of the porphyrin plane in the three derivatives are given in Figure 5 where the small φ values are quite evident.

Selected structural parameters and spin states for five- and six-coordinate [Fe^{II}(TpivPP)(L_1)(L_2)] imidazole derivatives are listed in Table 3. L_1 and L_2 denote the ligands on the hindered and unhindered sides of the porphyrin plane, respectively. We first consider the situation for six-coordinate complexes, all of which are low spin. It is noted that the two structures with anionic ligands, [Fe(TpivPP)(NO_2)(HIm)] and [Fe(TpivPP)(Im^-)(HIm)]$^-$, have the smallest φ_2 angles. Even if these two are not considered, it is perhaps surprising to find that the other complexes have φ_2 angles in the very

(36) Collins, D. M.; Countryman, R.; Hoard, J. L. *J. Am. Chem. Soc.* **1972**, *94*, 2066.
(37) Safo, M. K.; Walker, F. A.; Raitsimring, A. M; Walters, W. P.; Dolata, D. P.; Debrunner, P. G.; Scheidt, W. R. *J. Am. Chem. Soc.* **1994**, *116*, 7760.
(38) Walker, F. A.; Nasri, H.; Turowska-Tyrk, H.; Mohanrao, K.; Watson, C. T.; Shokhirev, N. V.; Debrunner, P. G.; Scheidt, W. R. *J. Am. Chem. Soc.* **1996**, *118*, 12109.
(39) Moore, K. T.; Fletcher, J. T.; Therien, M. J. *J. Am. Chem. Soc.* **1999**, *121*, 5196.
(40) Grinstaff, M. W.; Hill, M. G.; Birnbaum, E. R.; Schaefer, W. P.; Labinger, J. A.; Gray, H. B. *Inorg. Chem.* **1995**, *34*, 4896.
(41) *CrystalMaker* Version 7.2.3; CrystalMaker Software: Bicester, Oxfordshire OX26 3TA, England, 2007.

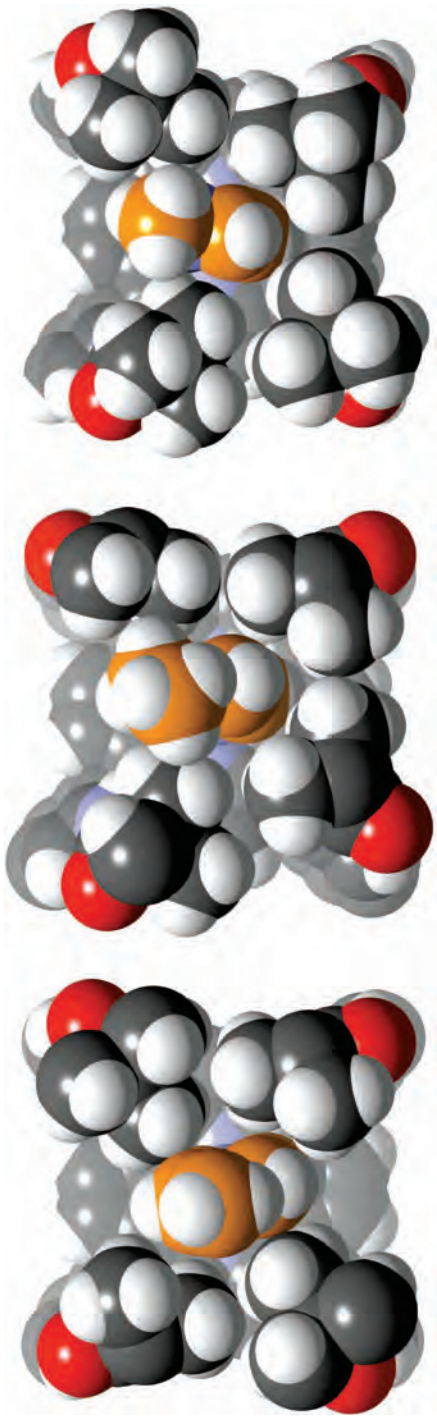

Figure 4. Spacing-filling diagrams (view perpendicular to the porphyrin plane) of [Fe(TpivPP)(1-MeIm)$_2$] (top), [Fe(TpivPP)(1-EtIm)$_2$] (middle), and [Fe(TpivPP)(1-VinylIm)$_2$] (bottom), showing the pocket porphyrin side (Carbon, dark grey; imidazole carbon, brown; Hydrogen, light grey; Nitrogen, blue; Oxygen, red; drawn with Crystalmaker[41]).

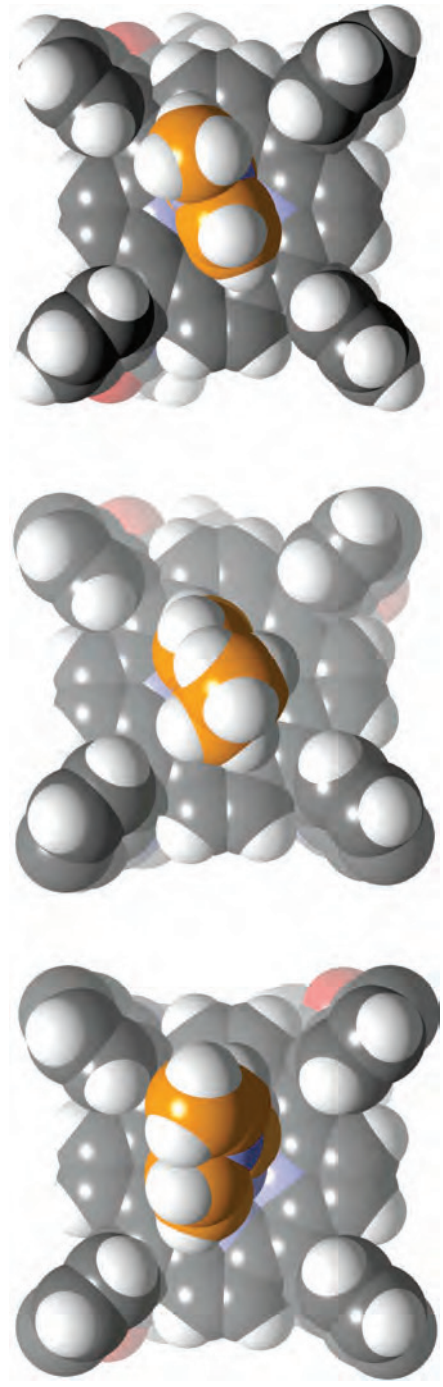

Figure 5. Spacing-filling diagrams (view perpendicular to the porphyrin core) of [Fe(TpivPP)(1-MeIm)$_2$] (top), [Fe(TpivPP)(1-EtIm)$_2$] (middle), and [Fe(TpivPP)(1-VinylIm)$_2$] (bottom), showing the unhindered porphyrin side (180 °; rotated from Figure 4) (Carbon, dark grey; imidazole carbon, brown; Hydrogen, light grey; Nitrogen, blue; Oxygen, red; drawn with Crystalmaker[41]).

narrow range of 20–24.5°. This result indicates that the imidazole on the unhindered porphyrin side is very likely to have a dihedral angle $\leq \sim 22°$ with the closest Fe−N_p axis, irrespective of the ligands on the opposite side. This is seen even for five-coordinate high-spin [Fe(TpivPP)(2-MeHIm)], where the bulky imidazole has a φ_2 angle of 22.8°.

These observations allow us to rationalize the absolute orientation of the imidazole ligands on the unhindered porphyrin plane side. However, these absolute orientations could equally lead to either relative parallel or relative

(42) Steffen, W. L.; Chun, H. K.; Hoard, J. L.; Reed, C. A. *Abstracts of Papers*, 175th National Meeting of the American Chemical Society, Anaheim, CA, March 13, 1978; American Chemical Society: Washington, DC, 1978; INOR 15.
(43) Silvernail, N. J.; Noll, B. C.; Scheidt, W. R. *Acta Crystallogr., Sect. E* **2005**, *E61*, m1201.

Table 3. Selected Structural Parameters for [Fe(TpivPP)(L_1)(L_2)] Imidazole Derivatives[a,b]

complex	spin state	Δ[c,d]	(Fe−N_p)$_{av}$[e]	Fe−L_1[d]	Fe−L_2[d]	φ_1[f,g]	φ_2[f,g]	θ[f,h]	ref.
Five-Coordinate									
[Fe(TpivPP)(2-MeHIm)]	HS	−0.43	2.072(2)		2.095(6)		22.8		49
[Fe(TpivPP)(2-MeIm$^-$)]$^-$	HS	0.65	2.106(20)	2.002(15)		14.7			50
Six-Coordinate									
[Fe(TpivPP)(1-MeIm)$_2$]	LS	0.04	1.9924(28)	1.9958(19)	1.9921(18)	8.5	21.1	77.2	tw
[Fe(TpivPP)(1-EtIm)$_2$]	LS	0.05	1.993(6)	2.0244(18)	1.9940(19)	6.6	20.7	64.3	tw
[Fe(TpivPP)(1-VinylIm)$_2$]	LS	0.05	1.988(5)	1.9979(19)	1.9866(18)	11.2	24.5	78.6	tw
[Fe(TpivPP)(O_2)(2-MeIm)]	LS	−0.11	1.996(2)	1.898(7)	2.107(4)	42.9,43.3	22.2	24.4,69.4	49
[Fe(TpivPP)(O_2)(1-MeIm)]	LS	0.02	1.98(1)	1.75(2)	2.07(2)	41.7,42.4	20	27.4,62.9	51,52
[Fe(TpivPP)(Im$^-$)(HIm)]$^-$	LS	0.01	1.995(9)	1.930(5)	1.953(5)	25.1	11.7	36.8	50
[Fe(III)(TpivPP)(NO_2)(HIm)]	LS	−0.01	1.970(4)	1.949(10)	2.037(10)	37	16.4	69	53

[a] Estimated standard deviations are given in parentheses. [b] L_1 denotes the ligand in the pocket of the porphyrin, L_2 denotes the ligand on the unhindered porphyrin side. [c] Displacement of iron atom from the 24-atom mean plane, a positive value is toward to the hindered porphyrin side. [d] Value in Å. [e] Average value in Å. [f] Value in degree. [g] Dihedral angle between the planes defined by the closest N_p−Fe−N_{ax} and the ligand plane. [h] Dihedral angle between two axial ligands.

perpendicular orientations of the axial imidazole pairs. What bonding feature gives the observed relative perpendicular orientation to three distinct picket fence derivatives?

Prior density functional theory (DFT) calculations have suggested that [Fe(II)(Porph)($L)_2$] complexes, especially when the axial ligands are imidazoles, do not have a strong orientational preference.[54,55] The two idealized ligand orientations, relative parallel versus relative perpendicular, are calculated to be isoenergetic conformers to within 1 kcal/mol. These calculations start by assuming that the projection of the first imidazole ligand will bisect an equatorial N_p−Fe−N_p angle yielding a φ angle of ~45°, much larger than those observed here. In an earlier study, Scheidt and Chipman[35] had suggested that a metal pπ−imidazole pπ interaction would favor eclipsed orientations for both five- and six-coordinate imidazole-ligated species.

The values of the axial Fe−N_{Im} bonds given in Table 2 suggest that, in the picket fence derivatives with relative perpendicular orientations, the axial bonding is slightly stronger than the four imidazole-ligated complexes with relative parallel orientations. The axial distances found for the relative parallel orientation species are systematically larger.[35,36] However, the differences are marginal and are certainly not significant at the three sigma level. Nonetheless, the systematic orientational behavior of the picket fence derivatives suggests an underlying effect. The most reasonable explanation for the apparently systematic effect in the picket fence porphyrin derivatives is that a very modest π-bonding between the imidazole and iron will be maximized only if the two axial ligands have a relative perpendicular orientation. Like the differences in the axial bond lengths, the effect must be a very modest one. The evidence presented here suggests that the effect starts with the enforced orientation of the axial ligand nearly eclipsing a coordinating Fe−N_p bond. The steric effects of the pickets prevents the rotation of the imidazole. Such rotations are known to be quite rapid in a number of model heme complexes in homogeneous solution.[56] This suggests that any further theoretical studies of axial ligand orientation effects should include consideration of the absolute as well as the relative ligand orientation.

Mössbauer Spectra. Mössbauer spectra were measured for the three new complexes in the solid state from room temperature to 20 K; the 200 K spectra are illustrated in Figure 6. The spectra are very similar and consist of a single quadrupole doublet at all temperatures. The quadrupole splitting decreases slightly with decreasing temperature with a maximum value of 1.07 mm/s at room temperature and a minimum of 0.99 mm/s at 20 K. The isomer shift increases slightly from 0.35 to 0.45 mm/s. Both the quadrupole splitting and the isomer shift values are those expected for low-spin iron(II) complexes.

Table 4 shows the Mössbauer data observed for the current complexes and the values observed for all known, related six-coordinate low-spin species. An examination of all quadrupole splitting values shows that almost all of these species have quadrupole splitting values in the range of 1.0–1.2 mm/s, with the pyridine derivatives having slightly higher values than those of the imidazoles. Only one set of imidazole derivatives, those with a sterically bulky 2-substituent on the imidazole ligand, are seen to have quadrupole splitting constants greater than ~1.60 mm/s. Only one such

(44) Li, N.; Petricek, V.; Coppens, P.; Landrum, J. *Acta Crystallogr., Sect. C* **1985**, *C41*, 902.
(45) Li, N.; Coppens, P.; Landrum, J. *Inorg. Chem.* **1988**, *27*, 482.
(46) Radonovich, L. J.; Bloom, A.; Hoard, J. L. *J. Am. Chem. Soc.* **1972**, *94*, 2073.
(47) Scheidt, W. R.; Noll, B. C. *Acta Crystallogr., Sect. E* **2006**, *E62*, m1892.
(48) Hiller, W.; Hanack, M.; Mezger, M. G. *Acta Crystallogr., Sect. C* **1987**, *C43*, 1264.
(49) Jameson, G. B.; Molinaro, F. S.; Ibers, J. A.; Collman, J. P.; Brauman, J. I.; Rose, E.; Suslick, K. S. *J. Am. Chem. Soc.* **1980**, *102*, 3224.
(50) Mandon, D.; Ott-Woelfel, F.; Fischer, J.; Weiss, R.; Bill, E.; Trautwein, A. X. *Inorg. Chem.* **1990**, *29*, 2442.
(51) Collman, J. P.; Gagne, R. R.; Reed, C. A.; Robinson, W. T.; Rodley, G. A. *Proc. Natl. Acad. Sci. U.S.A.* **1974**, *71*, 1326.
(52) Jameson, G. B.; Rodley, G. A.; Robinson, W. T.; Gagne, R. R.; Reed, C. A.; Collman, J. P. *Inorg. Chem.* **1978**, *17*, 850.
(53) Nasri, H.; Wang, Y.; Huynh, B. H.; Walker, F. A.; Scheidt, W. R. *Inorg. Chem.* **1991**, *30*, 1483.
(54) Medakovic, V.; Zaric, S. D. *Inorg. Chim. Acta* **2003**, *349*, 1.
(55) Ghosh, A.; Gonzales, E.; Vangberg, T. *J. Phys. Chem. B* **1999**, *103*, 1363.
(56) (a) Nakamura, M.; Groves, J. T. *Tetrahedron* **1984**, *44*, 3225. (b) Walker, F. A.; Simonis, U. *J. Am. Chem. Soc.* **1991**, *113*, 8652. (c) Shokhirev, N. V.; Shokhireva, T. Kh.; Polam, J. R.; Watson, C. T.; Raffii, K.; Simonis, U.; Walker, F. A. *J. Phys. Chem. A* **1997**, *101*, 2778. (d) Momot, K. I.; Walker, F. A. *J. Phys. Chem. A* **1997**, *101*, 2787. (e) Nakamura, M.; Tajima, K.; Tada, K.; Ishizu, K.; Nakamura, N. *Inorg. Chim. Acta* **1994**, *224*, 113. (f) Polam, J. R.; Shokhireva, T. Kh.; Raffii, K.; Simonis, U.; Walker, F. A. *Inorg. Chim. Acta* **1997**, *263*, 109.

Table 4. Selected Mössbauer Parameters for [Fe(II)(Porph)(L)$_2$] Derivatives

complex	ΔE_Q[a]	δ_{Fe}[a]	sample phase	T, K	θ[b]	conf.[c]	ref.
[Fe(TpivPP)(1-MeIm)$_2$]	0.99	0.44	cryst solid	20	77.2	near-Pla	tw
	1.00	0.43		100			
	1.02	0.42		200			
	1.05	0.35		298			
[Fe(TpivPP)(1-EtIm)$_2$]	1.03	0.45	cryst solid	20	64.3	near-Pla	tw
	1.04	0.44		100			
	1.05	0.42		200			
	1.07	0.37		298			
[Fe(TpivPP)(1-VinylIm)$_2$]	1.02	0.43	cryst solid	20	78.6	near-Pla	tw
	1.02	0.42		100			
	1.03	0.41		200			
	1.07	0.35		298			
[Fe(TMP)(2-MeHIm)$_2$]	1.70	0.42	cryst solid	100	82.4/84.4	Ruf	27
[Fe(TPP)(1-MeIm)$_2$]	1.07	0.47	cryst solid	77	0	near-Pla	28
[Fe(TPP)(1-AcIm)$_2$]	0.97	0.45	cryst solid	77	*d*	*d*	28
[Fe(TPP)(1-VinylIm)$_2$]	1.02	0.45	cryst solid	77	0	near-Pla	28
[Fe(TPP)(1-BzylIm)$_2$]	1.02	0.45	cryst solid	77	0	near-Pla	28
[Fe(TPP)(1-SiMe$_3$Im)$_2$]	1.04	0.46	cryst solid	77	*d*	*d*	28
[Fe(TPP)(Py)$_2$]	1.15	0.40	cryst solid	77	0	near-Pla	59
[Fe(OEP)(Py)$_2$]	1.13	0.46	cryst solid	4.2	*d*	*d*	60
[Fe(TMP)(1-MeIm)$_2$]	1.11	0.43	cryst solid	120	*d*	*d*	26
[Fe(TMP)(4-CNPy)$_2$]	1.13	0.41	cryst solid	120	0	near-Pla	26
[Fe(TMP)(3-ClPy)$_2$]	1.23	0.43	cryst solid	120	0	near-Pla	26
[Fe(TMP)(4-MePy)$_2$]	1.12	0.42	cryst solid	120	0	near-Pla	26
[Fe(TMP)(4-NMe Py)$_2$]	1.27	0.36	cryst solid	120	0	near-Pla	26
[Fe(TMP)(2-MeHIm)$_2$]	1.64	0.39	frozen soln	77	*e*	*e*	58
[Fe(TMP)(1,2-Me$_2$ Im)$_2$]	1.73	0.39	frozen soln	77	*e*	*e*	58
[Fe(OEP)(2-MeHIm)$_2$]	1.67	0.34	frozen soln	77	*e*	*e*	58
[Fe(OEP)(4-NMe$_2$Py)$_2$]	1.02	0.45	frozen soln	77	*d*	*d*	58
[Fe(OEP)(4-CNPy)$_2$]	1.10	0.32	frozen soln	77	*d*	*d*	58
[Fe(OEP)(1-MeIm)$_2$]	0.96	0.46	frozen soln	77	*d*	*d*	58

[a] mm/s. [b] Dihedral angle between two axial ligands. [c] Predominant core conformation contribution; Pla, planar; Ruf, ruffled. [d] Not determined, presumed parallel and planar. [e] Not determined, presumed perpendicular and ruffled.

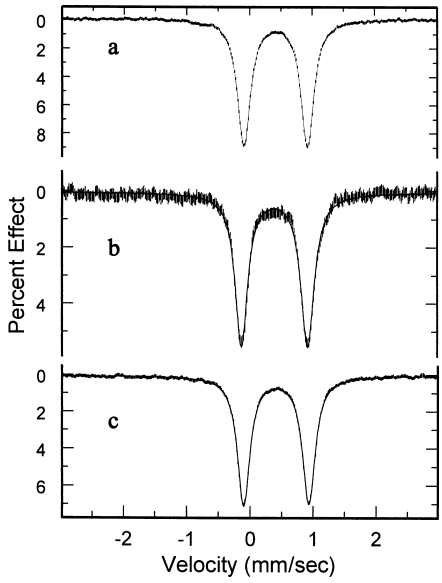

Figure 6. Mössbauer spectra in 500 mT field of (a) [Fe(TpivPP)(1-MeIm)$_2$], (b) [Fe(TpivPP)(1-EtIm)$_2$], and (c) [Fe(TpivPP)(1-VinylIm)$_2$] at 200 K.

species showing a large quadrupole doublet has been structurally characterized, the [Fe(TMP)(2-MeHIm)$_2$] derivative.[27] The two independent molecules in the structure both had the two axial ligands in a relative perpendicular arrangement. We suggested that the quadrupole splitting value for low-spin bis(planar axial ligand) iron(II) systems was sensitive to the relative orientation of the two axial ligands.[27] Thus, larger values of the quadrupole splitting ($\geq$1.5 mm/s) result from the presence of relative perpendicular ligand orientations, whereas lower values ($\leq$1.25 mm/s) result from relative parallel orientations. On the other hand, Grodzicki et al.[57] had suggested that the large quadrupole splitting constant was the result of porphyrin core ruffling. Their conclusion was based on the presumed ruffled core conformation for a series of complexes studied in frozen solution;[58] no crystal structure data were then available.

The new picket fence derivatives with their relative perpendicular axial ligand orientations and nearly planar cores allow us to examine the issue further. Table 4 displays, in addition to the Mössbauer quadrupole splitting and the isomer shift values, the relative axial ligand orientation (θ) and the core conformations for all bis-ligated derivatives. The entries in the table clearly show that the common geometric factor for a large quadrupole splitting constant is a ruffled core conformation and not ligand orientation. Moreover, since the quadrupole splitting values are most sensitive to d-electron configuration, it is clear that the aggregate d-electron configuration in the picket fence derivatives and the imidazole-ligated derivatives with parallel axial ligand orientations are very similar, and consistent with the conclusion that a major influence in defining the eclipsed axial imidazole orientations is an iron pπ−imidazole pπ interaction.[35]

(57) Grodzicki, M.; Flint, H.; Winkler, H.; Walker, F. A.; Trautwein, A. X. *J. Phys. Chem. A* **1997**, *101*, 4202.
(58) Polam, J. R.; Wright, J. L.; Christensen, K. A.; Walker, F. A.; Flint, H.; Winkler, H.; Grodzicki, M.; Trautwein, A. X. *J. Am. Chem. Soc.* **1996**, *118*, 5272.

Summary

Three bis(imidazole-ligated)iron(II) "picket fence" porphyrinates have been prepared and characterized by X-ray structure determinations and multitemperature Mössbauer spectroscopy. The steric demands on the picket side of the porphyrin require that the projection of the imidazole plane on that side to nearly eclipse an $Fe-N_p$ bond direction. All three derivatives have the two axial ligand planes with a relative perpendicular orientation. This is the first time that such a ligand orientation with a nearly planar porphyrin core and unhindered axial ligands has been observed and may result from the restriction of the rotation of the axial ligand on one side of the porphyrin plane. Mössbauer spectra were obtained for all three derivatives. A comparison of the values obtained demonstrated that the quadrupole splitting values are sensitive to porphyrin core conformation and not to the relative axial ligand orientation.

(59) Kobayashi, H.; Maeda, Y.; Yanagawa, Y. *Bull. Chem. Soc. Jpn.* **1970**, *43*, 2342.
(60) Dolphin, D.; Sams, J. R.; Tsin, T. B.; Wong, K. L. *J. Am. Chem. Soc.* **1976**, *98*, 6970.

Acknowledgment. We thank the National Institutes of Health for support of this research under Grant GM-38401 (W.R.S). We thank the NSF for X-ray instrumentation support through Grant CHE-0443233.

Supporting Information Available: Crystallographic data in CIF format, figures with ORTEP diagrams, and tables with complete crystallographic details, atomic coordinates, bond lengths, bond angles, and anisotropic/isotropic displacement parameters (PDF). This material is available free of charge via the Internet at http://pubs.acs.org.

IC702498C